

WET-WEATHER-EFFECTIVE BICYCLE RIM BRAKE:

A PRODUCT-DEVELOPMENT EXERCISE

by

BRIAN DONALD HANSON

Submitted in Partial Fulfillment

of the Requirements for the

Degree of Master of Science

at the

MASSACHUSETTS INSTITUTE OF TECHNOLOGY

June, 1971

Signature of Author
Department of Mechanical Engineering, May 14, 1971

Certified by .

Thesis Supervisor

Accepted by .

Chairman, Departmental Committee
on Graduate Students

Archives



Wet-weather-effective Bicycle Rim Brake:

A Product-development Exercise

by Brian Donald Hanson

Submitted to the Department of Mechanical Engineering
on May 14, 1971, in partial fulfillment of the requirement
for the degree of Master of Science.

A wet-weather-effective bicycle rim brake to replace present bicycle rim brakes was developed in the following manner. Various friction materials were tested, and one was chosen whose friction characteristics (on a bicycle rim surface) were least affected by water. A mechanism was required which takes into account the mechanical and frictional characteristics of the friction material, the highly force- and stroke-limited nature of the handgrip-cable input, requirements for one-point pivot mounting, wear of the friction material, and general weight and reliability considerations.

Nonlinear, servo-assist and dual-mode mechanisms were considered. Simplicity of design and construction favored the dual-mode mechanism, of the slider-and-lever variety, and two prototypes were constructed. The second of these prototypes underwent several weeks of field-testing, and preliminary results are favorable. Further study is recommended concerning the effectiveness of negative force feedback, increased overall compliance, friction material area, hydraulic rather than mechanical actuation, and mass-productibility considerations.

Thesis Supervisor: David Gordon Wilson

Title: Associate Professor of Mechanical Engineering

The author wishes to thank the following personnel for valuable technical assistance and encouragement: Mr. Ray Johnson and staff of the Mechanical Engineering Department machine shop; Mr. Fred Anderson of the Materials Processing Laboratory; and Mr. Clarence Christiansen and Mr. William Wingfield of the Student Machine Shop.

This project was supported in part by the Fred B. Asche Fund and the Ella Lyman Cabot Trust, through the courtesy of Dr. Paul Dudley White.

CONTENTS

Abstract	2
Acknowledgments	3
List of Illustrations	5
Introduction	6
Friction Tests	9
Design Decisions	15
Prototype Construction and Testing	20
Recommendations for Further Work	23
Bibliography	26
Appendix A. Friction Material Specimen Mount	31
Appendix B. Processing of Experimental Data	32
Appendix C. Tabulated Experimental Results	34
Appendix D. Nonlinear Mechanisms	36
Appendix E. Servo-assist Mechanisms	39
Appendix F. Dual-mode Mechanisms; Prototypes	41

ILLUSTRATIONS

1. Experimental Setup	27
2. Friction-material Specimen Mount	27
3. Friction-material Specimen in Mount	28
4. Friction material in Contact with Rim	28
5. First Prototype Installed on Bicycle	29
6. Detail of First Prototype	29
7. Second Prototype Installed on Bicycle	30
8. Detail of Second Prototype	30
9. Forces and Geometry of Specimen Mount	31
10. Graphical Output for Typical Experimental Run	33
11. Experimental Results	34
12. Geometry of "Door-closer" Linkage	36
13. Characteristics of "Door-closer" Linkage	36
14. Geometry of Simple Toggle	37
15. Characteristics of Simple Toggle	37
16. Geometry of Stepped Toggle	38
17. Characteristics of Stepped Toggle	38
18. Roller-and-screw Servo	39
19. Pilot-shoe-and-wedge Servo	40
20. First Prototype	41
21. Forces and Geometry of Self-locking Slider	42
22. Second Prototype	43
23. Possible Production Version of Second Prototype	44

INTRODUCTION

Background

One approach to the problem of urban traffic congestion is to try to shift a significant fraction of the motoring public to bicycles for short-range personal transport. Much official enthusiasm has been recently directed towards bicycling, and a relatively modest further effort at publicity and assistance to bicyclists could put a substantial dent in the number of intraurban auto trips, under favorable weather conditions.

However, as is well known, traffic jams occur in rain and snow as well as in sunshine. For bicycles to alleviate this year-round problem, they must be modified or redeveloped to be attractive in all seasons as an alternative to automobiles.

The problem

In fair weather or foul, a bicycle rider is seriously exposed to collision dangers. Much of this problem is due to the present most-popular rim brakes, which are often only marginally effective under normal conditions, and dangerously poor in the wet. An additional deficiency is that the friction blocks wear excessively in heavy use, and adjustment and replacement are difficult.

To develop a bicycle brake with significantly greater wet-capability than present varieties, at no sacrifice of

reliability and maintainability (which are sufficiently poor already), is the goal of this program.

Previous work

Asbell (1) investigated various brake-block materials' behavior on bicycle-rim surfaces, wet and dry. The most favorable material, automotive Lockheed-brake friction material, experienced a 60 to 70% drop in coefficient of sliding friction with changes from dry to wet conditions.

Hanson (2) substantiated the above result; in addition, he determined the practical limit to friction-material pressure on a bicycle-wheel rim, and established the drop in friction to be independent of pressure within that limit. The dynamics of the dry-to-wet and wet-to-dry transitions, and the influence of friction-material characteristics on brake-mechanism design, were also considered.

Possible approaches

The goal of effective, consistent bicycle braking may be approached from a variety of directions. For rim brakes, various wheel materials and rim surfaces may be explored, as well as brake-block materials and actuation schemes (including hydraulic and power-assist). Sealed hub-type brakes have inherent all-weather capability; however, weight and cost problems, residual drag when disengaged,

and handgrip-compatibility difficulties have prevented their being factory-installed on front wheels (where effective braking is most critical).

Other areas of possible interest include nonfrictional braking, either electrically via hysteresis or eddy-current generation, or regeneratively via energy-storage (perhaps as part of a fluid power transmission system).

Present approach

The first problem encountered in undertaking any project is that of sufficiently limiting the scope of the project so that it may be adequately treated in the time allotted. To this end, the following decisions were made:

1. The result or output of this project will be a mechanism, bolted-on in place of existing caliper-brakes on current popular street bicycles (Raleigh and Phillips 3-speed, etc.) and on derailleur-equipped touring bicycles, with steel wheels only.

2. The mechanism must accept a handgrip-and-cable input.

3. No external energy sources (e.g. electrical, chemical) are permitted, save the bicycle's own forward motion.

FRICITION TESTS

Necessity for friction tests

The original problem statement was qualitative: bicycle rim brakes are ineffective in wet weather. Instrumentation and experimentation are necessary for two reasons:

1. To verify the existence of; and determine the magnitude of, the existing problem; and
2. To determine the effectiveness of solution attempts.

This experimentation may take two forms:

1. Instrument a bicycle and run it under actual conditions;
2. Simulate conditions in a laboratory.

The latter of these forms was chosen because power and weight restrictions, plus lack of portable equipment, made instrumenting a bicycle impractical. Stationary equipment and laboratory space, on the other hand, were readily available.

Goals of friction tests

The first step towards a solution of the problem of wet-weather braking is to select the friction material which undergoes the smallest relative drop in friction characteristics when it is wetted. If the absolute fric-

tion characteristics of the selected material are sufficiently high, the material will be tried in a standard caliper mechanism; if not, another mechanism will be built which takes advantage of the characteristics (friction and otherwise) of the material.

Of the materials to be investigated, several have friction characteristics published for carefully-controlled conditions, dry and in oil, on cast-iron and uncoated steel surfaces.(3) No data are available from brake manufacturers involving either the presence of water or the use of plated or nonferrous surfaces.(4) Thus the determination of the most favorable friction material must be made on the basis of friction tests which we conduct.

Setup and procedure (first series of experiments)

The heart of the test apparatus was a 30-inch lathe in Room 1-014 (Fig.1.). A chromium-plated steel bicycle wheel, with spokes and hub, was chucked into the lathe, which was capable of 110,190 and 330 rpm (10, 17 and 30 mph, respectively).

For measurement of forces, a Cook, Smith Associates three-component-force machine-tool dynamometer was mounted in the tool compound of the lathe; strain gauges in the dynamometer were excited by, and their output amplified

and recorded by, a Sanborn 321 recording oscillograph. Two of the three components of force were handled, corresponding to normal and tangential forces on the brake material.

To hold the brake material specimen in the dynamometer, a fixture was fabricated consisting of two sections. One section held the brake material; the other was clamped into the dynamometer. Contact between sections was through ball-bearing rollers, permitting relative motion normal to the plane of the wheel, and restricting motion in other directions. Compliance in the direction of relative motion was governed by a die-spring of stiffness 192 lbf/in.

Each experimental run consisted of the following:

1. Brake material specimen selected and mounted in the fixture
2. Wheel rotating at selected speed, and recorder running
3. Wheel and specimen wetted from a squeeze bottle, or left dry as required
4. Specimen brought up to wheel, and normal force increased to some maximum value (Fig.4)
5. Specimen withdrawn after a few seconds (for a dry wheel), or after dry-friction behavior is recovered (for a wet wheel)

6. Lathe and recorder stopped; wheel temperature noted qualitatively; wheel allowed to cool to ambient temperature.

The output of each experimental run was an annotated strip chart, on which were recorded (vs. time) two traces, one corresponding to normal force on the brake specimen (and on the dynamometer), the other corresponding to a moment on the dynamometer due to tangential force on the brake specimen (Fig.10).

Geometric problems and fixture redesign

When an effort was made to calculate tangential force, it was discovered that not enough was known geometrically to functionally relate normal force, tangential force, and moment. The location of the axis about which the dynamometer sensed moments was known horizontally from the calibration procedure, but was not known vertically. Furthermore, the location of the origin of the resultant force on the brake specimen was not known, since this depended on the distribution of pressure and shear stresses over the face of the specimen.

Consequently, it was decided to redesign the fixture so that the brake specimen could rotate about a pivot. Equilibrium requires that all moments about that pivot sum to zero, and therefore that the resultant force pass

through the pivot axis. It was also decided to make the pivot axis vertically adjustable, so that it could be placed at the same elevation as the moment axis of the dynamometer. The function relating normal force, tangential force and moment would be simplified, and the data-reduction task shortened.

The fixture was altered accordingly (Figs.2 and 3), and the height of the pivot axis was adjusted in the following manner:

1. A roller was substituted for the brake-specimen holder on the pivot axis, making the fixture able to transmit normal forces only.
2. The fixture was brought up to the wheel (not rotating) and some force applied. Moment was observed on the recorder.
3. Pivot-axis height was adjusted, and the above step repeated, until no moment was observed on application of normal force. At that point, the pivot axis of the fixture and the moment-sensing axis of the dynamometer were at equal elevations.

Subsequent experiments

Another sequence of experimental runs was made with the redesigned fixture, following the same procedure as the previous sequence. Raw output and data reduction for

a typical run are given in Appendix B, and tabulated results for the entire sequence are given in Appendix C.

Summary of results

On a chromium-plated steel wheel with a moderately-worn surface, a standard rubber caliper-brake friction block has a sliding coefficient of friction of unity when dry and 0.05 when wet -- a factor-of-twenty difference. Of the materials tested, Raybestos R-451 experienced the smallest relative change in friction characteristics; on the same wheel, this material has a sliding coefficient of 0.34 dry and 0.17 wet -- a factor-of-two difference, and an order-of-magnitude improvement over the existing material.

DESIGN DECISIONS

Performance requirements

Given the characteristics of the friction material to be used, the performance requirements of the brake mechanism, and the constraints the mechanism must obey, the task is to design and build the actual mechanism.

The friction material selected is Raybestos R-451, a rigid, molded, asbestos-reinforced automotive braking compound whose coefficient of friction on a bicycle wheel is 0.34 dry and 0.17 wet.

The brake mechanism must be capable of decelerating a 250-lbm bicycle-and-rider at $0.4g$, or about 13 ft/sec^2 , braking the front wheel only, with an input force at the handgrip of 50 lbf or less. This requires that the mechanism convert a 50-lbf input force to a tangential (braking) force of 100 lbf on the wheel rim (50 lbf for each of two friction blocks). Under wet conditions, this requires $50 \text{ lbf} / \mu$, or 300 lbf normal (applied) force to each friction block. To transform the 50-lbf input force to a 300-lbf normal force, the mechanism must have a mechanical advantage of 6.

However, in order to allow for wheel wobble and irregularities, a clearance of at least $1/8$ inch must be maintained between the wheel rim and the friction block on each side, for a total clearance of $1/4$ inch, when the brake mechanism is fully disengaged. A mechanism with a constant

mechanical advantage of 6 would require 1.5 inches of stroke at the input to take up this clearance, but only 1/2 inch of stroke is available at the handgrip cable. In addition, such a mechanism would require frequent adjustment for friction-material wear.

Thus an additional requirement must be set, that the mechanism not require excessive handgrip-cable travel to take up normal clearance before engaging the wheel rim.

Design alternatives

There are three possible routes to take in designing a mechanism to meet the above constraints:

1. Nonlinear linkage - A relatively small mechanical advantage in the clearance-takeup region increases with brake travel until it reaches the required magnitude at the point where the friction blocks come into contact with the wheel rim.

2. Servo assist - The forward motion of the wheel is used to supply the actuating energy to the mechanism.

3. Dual-mode mechanism - Two operating regimes exist, one of low mechanical advantage to take up clearance, the other of high mechanical advantage to supply the necessary normal force. Switching between the modes would occur when the friction blocks contact the wheel rim.

Nonlinear linkage

Geometry and characteristics of two representative

nonlinear mechanisms are given in Appendix D. Both mechanisms have the advantage of being simply constructed, and both have the disadvantage that at any given point in their operating regions the mechanical advantage is fixed; thus in each of these mechanisms, the region of highest mechanical advantage is also the region of greatest sensitivity to friction-material wear. Such mechanisms would consequently require frequent adjustment, or would have to have a self-adjusting feature added on.

Servo actuation

Two representative servo-actuated mechanisms are given in Appendix E, one featuring rotary actuation via an abrasive-coated roller against the tire-tread, the other being linearly actuated via a pair of pilot shoes engaging the wheel rim similarly to the main (braking) shoes. For both mechanisms, the input quantity acted upon is a force rather than a displacement (neglecting wear of roller or pilot shoes); regardless of the effective mechanical advantage, the only wear-sensitivity of the mechanism occurs at the pilot stage, where the mechanical advantage is roughly one. Friction-material wear at the main (braking) stage affects only the time required to take up friction-block clearance before braking actually begins.

Another advantage is that negative force-feedback can be employed in either of these mechanisms, resulting in a

tendency of the mechanism to generate a braking force proportional to the input force despite changes in friction conditions.

A potential disadvantage associated with negative feedback is the possibility that the resultant system may be dynamically unstable. The function of any braking system is to transform kinetic energy (usually into heat), but this energy can only too easily find its way into such spurious forms as noise and vibration, deformation and fracture of materials, and kinetic energy of flying fragments.

Reliability of operation and "tolerance for neglect" are two of the prime requirements a bicycle brake must fill. Both of these servo-actuated mechanisms would require periodic cleaning and lubrication in order to function properly, especially in releasing when the handgrip force is withdrawn.

Dual-mode

Another scheme for providing the necessary combination of clearance takeup and high mechanical advantage, is to have separate mechanisms for each task. One mechanism, of low mechanical advantage, would bring the friction blocks across the clearance space and into contact with the wheel rim; at that point the action would switch to another mechanism, of high mechanical advantage, to provide the necessary normal force to the friction blocks. In the simplest

case (see Appendix F), the first mechanism would be a slider, the second mechanism would be a simple lever, and switching would be accomplished by locking or jamming of the slider.

The primary advantage of this type mechanism is that each of the sets of mechanical characteristics the mechanism must have, exists only when it is actually needed. that is, the mechanism has a low (unity) mechanical advantage until it needs a high one. Consequently, it has a low sensitivity to geometric changes, i.e. friction-material wear, in the region where such changes would be experienced. Additionally, each of the modes (sliding and lever action) can be made to function reliably without maintenance.

The major potential disadvantage of a dual-mode mechanism concerns inter-mode switching. The mechanism depends for its success upon predictable, reversible and consistent switching from one mode to the other.

Practical considerations

In deciding which of the above three schemes to employ in the first prototype mechanism, several practical factors had to be considered:

1. Budget limitations (both time and money) required that all prototypes be built of scrap material by the author.

2. It was desired to execute at least one iteration

of the "build-test-evaluate-modify" development cycle in the limited time remaining, and that somewhere in this process a prototype would see daily use on a bicycle.

Upon first examination, the potential difficulties involved in employing a self-adjusting feature into a non-linear linkage, and the complicated nature of the servo-assist mechanisms, ruled in favor of the dual-mode mechanism for the first prototype.

PROTOTYPE CONSTRUCTION AND TESTING

First prototype

An assembly drawing of the first prototype appears in Fig. 20, Appendix F. The mechanism is single-ended (one side inert) for simplicity, and is of aluminum throughout. The friction material is Raybestos R-451, mounted in standard bicycle rim brake shoes. The sliding half of the mechanism does not itself lock; instead, a separate jamming link is provided. Intended operation is as follows:

1. Handgrip cable pulls sliding member inward until both friction blocks are firmly in contact with the wheel rim.
2. Further movement of the cable pulls both lever and jamming link inward against spring pressure. Pressure of spring from lever to jamming link overcomes spring from jamming link to slider. Jamming link moves inward until it locks.

3. At this point the lever is the only remaining part capable of movement. As the cable forces it inward, spring pressure to the jamming link is increased, providing more jamming effect as friction-block forces increase.

4. When the cable is released, the lever is the first to return to normal position; pressure of the spring from slider to jamming link forces link to unjam; and the centering/restoring spring forces slider outward until running clearance is restored between wheel rim and friction blocks.

Testing of first prototype

Shortness of project time prompted a decision to forego laboratory-testing of the prototype; directly after construction it was mounted in place of the front caliper-brake on the test bicycle, and field-testing was begun. Several difficulties were immediately encountered:

1. Asymmetric construction (and therefore imbalance) made centering the mechanism over the tire difficult; even when fully released, one side or the other rubbed the wheel rim, regardless of the adjustments made to the centering spring.

2. Jamming and unjamming were unreliable for all combinations of spring stiffnesses and pre-loadings tried.

The prototype is shown installed on the test bicycle in Fig. 5, and the reverse side of the prototype is shown in

detail in Fig. 6.

Proposed modifications

As a result of the tests conducted, the following modifications were suggested:

1. Eliminate the separate jamming link and alter the geometry of the slider so that it does its own jamming; also, move the point of force application (i.e. cable attachment) downward so that sliding will take place when desired.

2. Trim off all unnecessary metal on the operating side for the sake of balance and centering.

Construction of second prototype

Geometric derivations for a self-locking slider are given in Appendix F, followed by an assembly drawing of the second prototype. The self-locking slider has the following characteristic: Forces applied at the level of the lower sliding surface (i.e. those due to handgrip-cable or return spring) cause the slider to move freely in the direction of the force; and forces applied at the level of the friction blocks cause the slider to lock.

Testing of the second prototype

Initial tests revealed the modified prototype to be balanced, positive in operation, and consistent in behavior. Two drawbacks were noted: the mechanism's overall

structural stiffness caused fluctuations in rim width to result in grabbing at certain points on the wheel circumference, especially the weld. As the wheel (as well as the rest of the bicycle) was the cheapest available, the irregularities encountered represent an extreme. The other difficulty was that the mounting bolt securing the mechanism to the front fork was bent due to large, sudden braking reaction forces. A force-reaction member was installed which restrained forward motion of the mechanism; this alleviated the problem somewhat.

After a week of regular use, clearance between the slider and the frame of the mechanism increased to the point where the slider would occasionally fail to unjam. (Theory predicted that jamming and unjamming would be unaffected by clearance.) A thicker top block was fabricated and installed on the slider, and the problem was eliminated.

Overall and detail views of the second prototype, installed on the test bicycle, are shown in Figs. 7 and 8, respectively.

RECOMMENDATIONS FOR FURTHER WORK

As previously stated, the braking force developed by the prototype mechanism varies during brake-application with fluctuations in the wheel-rim width. The resultant grabbing tendency is attributable to the overall stiffness of the mechanism (of the order 10^4 lbf/in at the friction-

block faces). Two means are suggested to alleviate this difficulty: reduced stiffness and negative force feedback. Both of these methods, especially the latter, should be investigated with respect to their effects on the mechanism's sensitivity to rim irregularities, as well as on overall consistency of behavior and on reliability.

While the metal-on-metal friction behavior, depended upon for locking and unlocking of the slider, has been consistent in tests so far, it is not known what the long-term (1 year or more) effects of wear, oxidation and foreign substances will be on that behavior. Alternative actuation schemes immune to environmental effects (e.g. hydraulic actuation) should be examined for applicability to bicycle rim braking.

A British investigating team (5) observed improved braking performance with friction blocks of double the standard length. All tests in this project were carried out with standard-length (1.75 in) friction blocks. Further tests should be conducted to determine the effect of friction-block length on friction characteristics of both rigid and compliant friction materials.

Finally, the dual-mode brake mechanism should be scrutinized with an eye toward mass-production and marketability. Now that the principle has shown promise, other considerations such as manufacturing costs and eye appeal would enter into a complete redesign of the brake "package"

into a saleable item. One form this redesigned brake may take is shown in Fig. 23, Appendix F.

BIBLIOGRAPHY

- (1) Asbell, O.D., Jr., SB Thesis, MIT, June 1970
- (2) Hanson, B.D., SB Thesis, MIT, October 1970
- (3) Raybestos-Manhattan, Inc., Engineering Bulletin No.501
- (4) Raybestos Division of Raybestos-Manhattan, Inc.,
Paul Lee, Chief Sales Engineer, Letter of 23 Sept 1970
- (5) 1963 Road Safety Research Report, Road Research
Laboratory, Department of Scientific and Industrial
Research, British Ministry of Technology; Chapter 11,
"The Braking Performance of Vehicles"
- (6) Marks' Engineering Handbook, Seventh Edition (McGraw-
Hill, 1967), p.3.35



Fig. 1. Experimental setup in Room 1-014

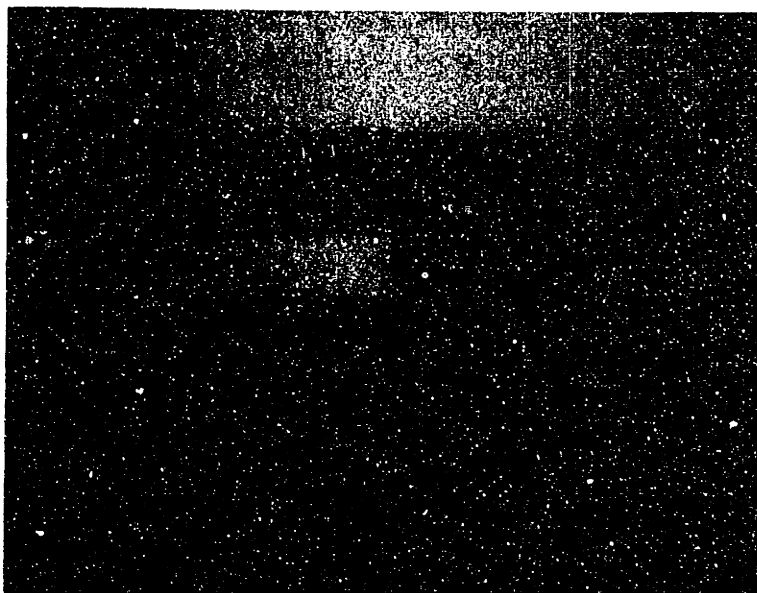


Fig. 2. Friction material specimen mounting fixture

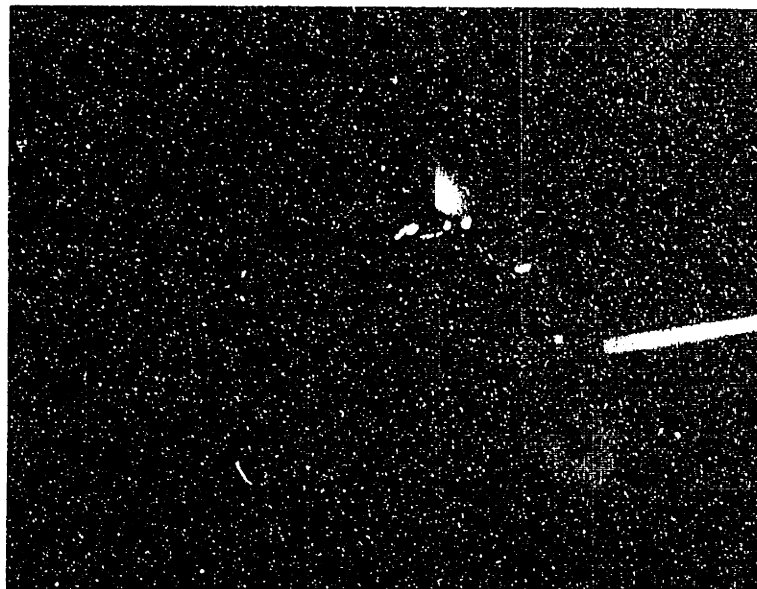


Fig. 3. Detail of friction material specimen in fixture

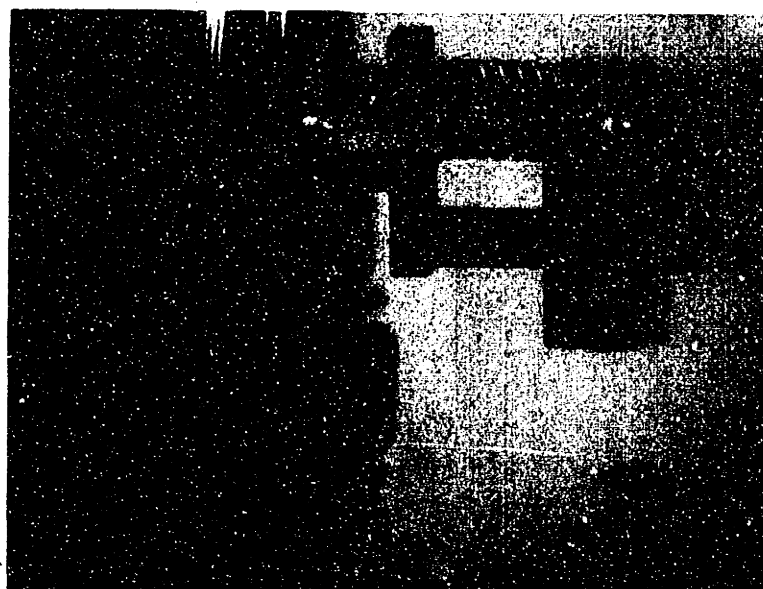


Fig. 4. Friction material in contact with rim

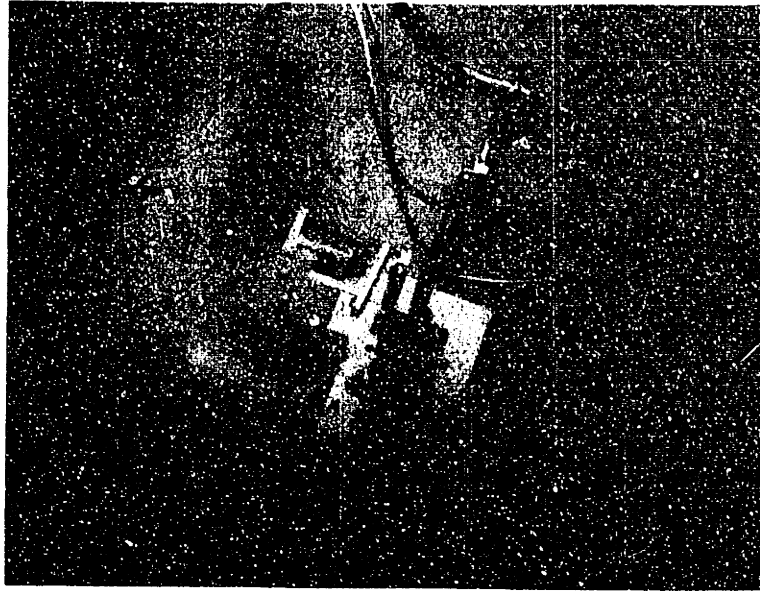


Fig. 5. First prototype installed on bicycle

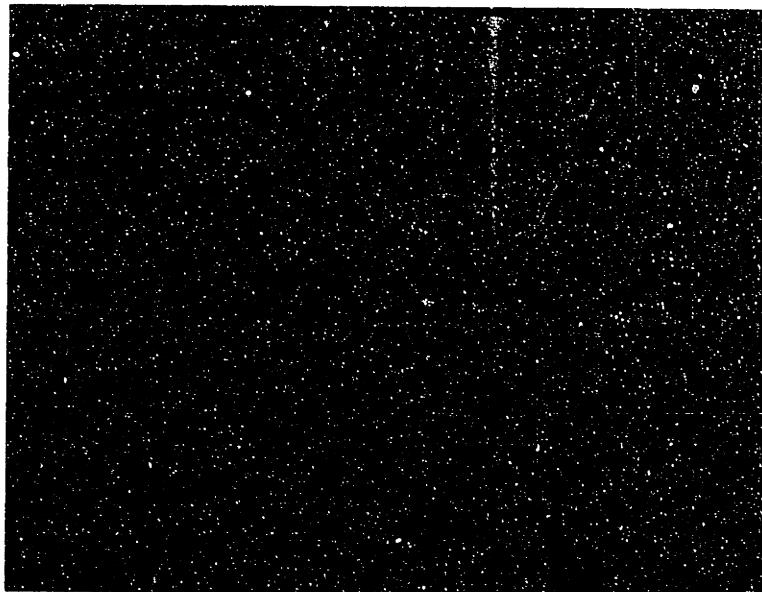


Fig. 6. Detail of first prototype

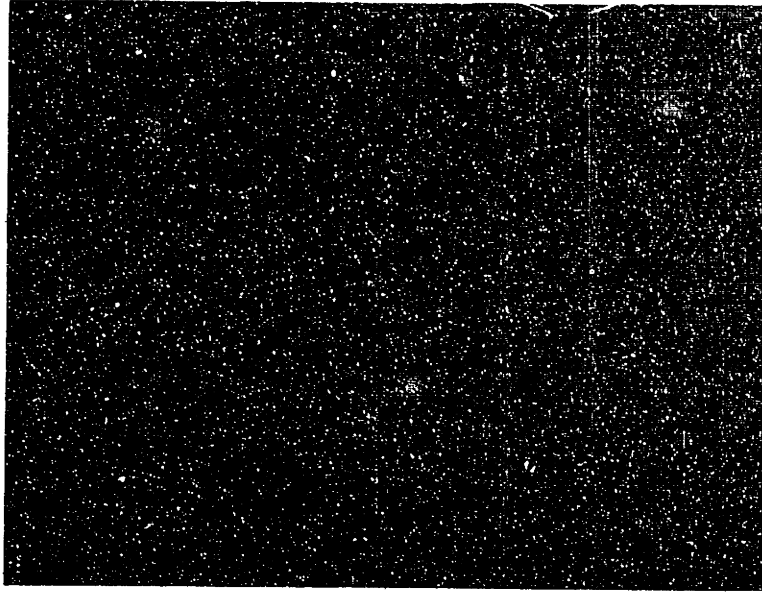


Fig. 7. Second prototype installed on bicycle

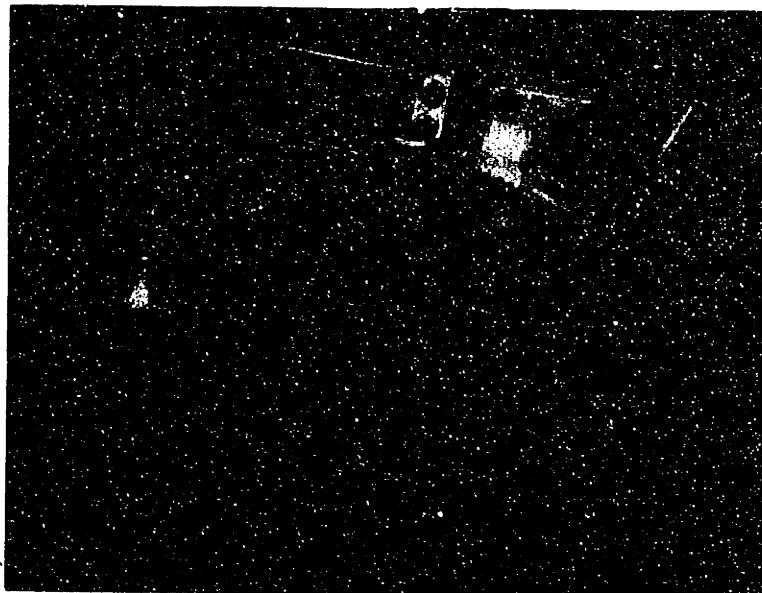


Fig. 8. Detail of second prototype

Appendix A. Geometry of friction material specimen mount

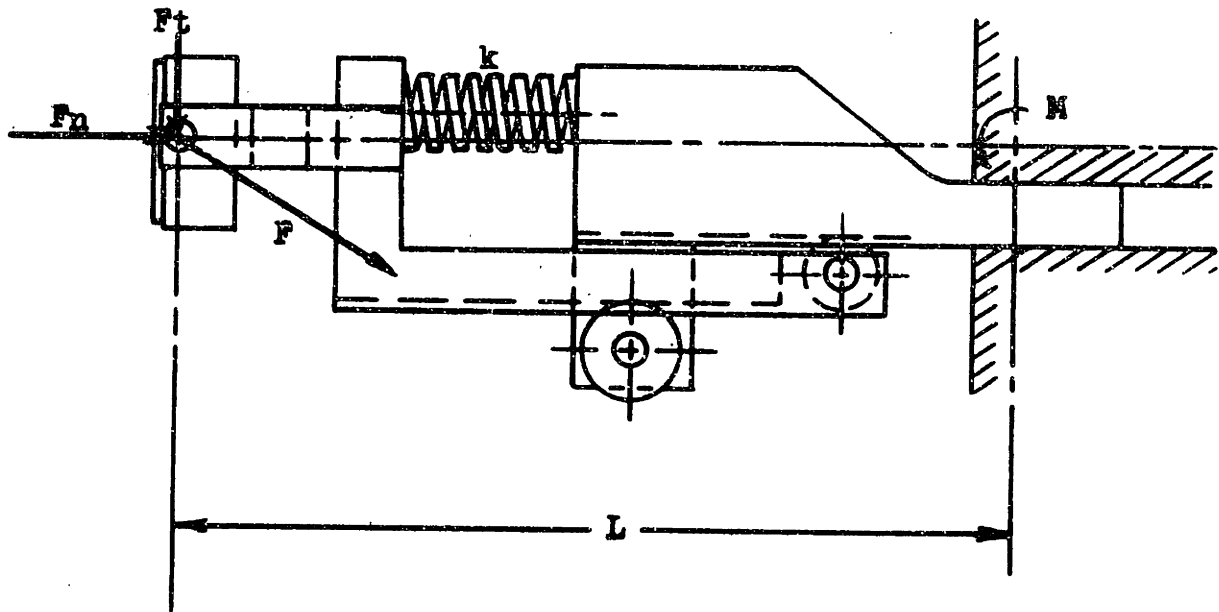


Fig. 9. Forces and geometry of specimen mount

$$L = L_0 - F_n/k ,$$

$$\text{Moment } M = F_t \cdot L .$$

The quantities detected by the equipment are M and F_n .

$$F_t = f(M, F_n)$$

$$F_t = \frac{M}{L_0 - F_n/k} .$$

Appendix B. Example of experimental data reduction

Run C-2 of 19 January 1971

Nature of run: Wet-dry

Flexible-mount data: $k = 192 \text{ lbf/in}$

Conversion factors, from calibration:

For F_n : $10.0 \text{ lbf/scale division}$

For M : $34.3 \text{ lbf-in/scale division}$

Geometric factor: $L_0 = 8.5 \text{ in}$

Derived formula: $F_t = \frac{M}{8.5 \text{ in} - (F_n/192 \text{ lbf/in})}$

Point (See Fig. 10.)	Observed		Converted		Calculated	
	F_n (scale div)	M	F_n (lbf)	M (lbf-in)	F_t (lbf)	μ
1 (wet start)	13	5	130	172	22	.17
2 (pre-recovery)	13	5	130	172	22	.17
3 (recovering)	13	6	130	206	26	.20
4 (")	13	7	130	240	31	.24
5 (")	13	8	130	274	35	.27
6 (")	13	9	130	309	39	.30
7 (recovered)	13	10	130	343	44	.34

Turns of wheel before onset of recovery: 30

Turns of wheel during recovery: 20

Total turns to recovery: 50

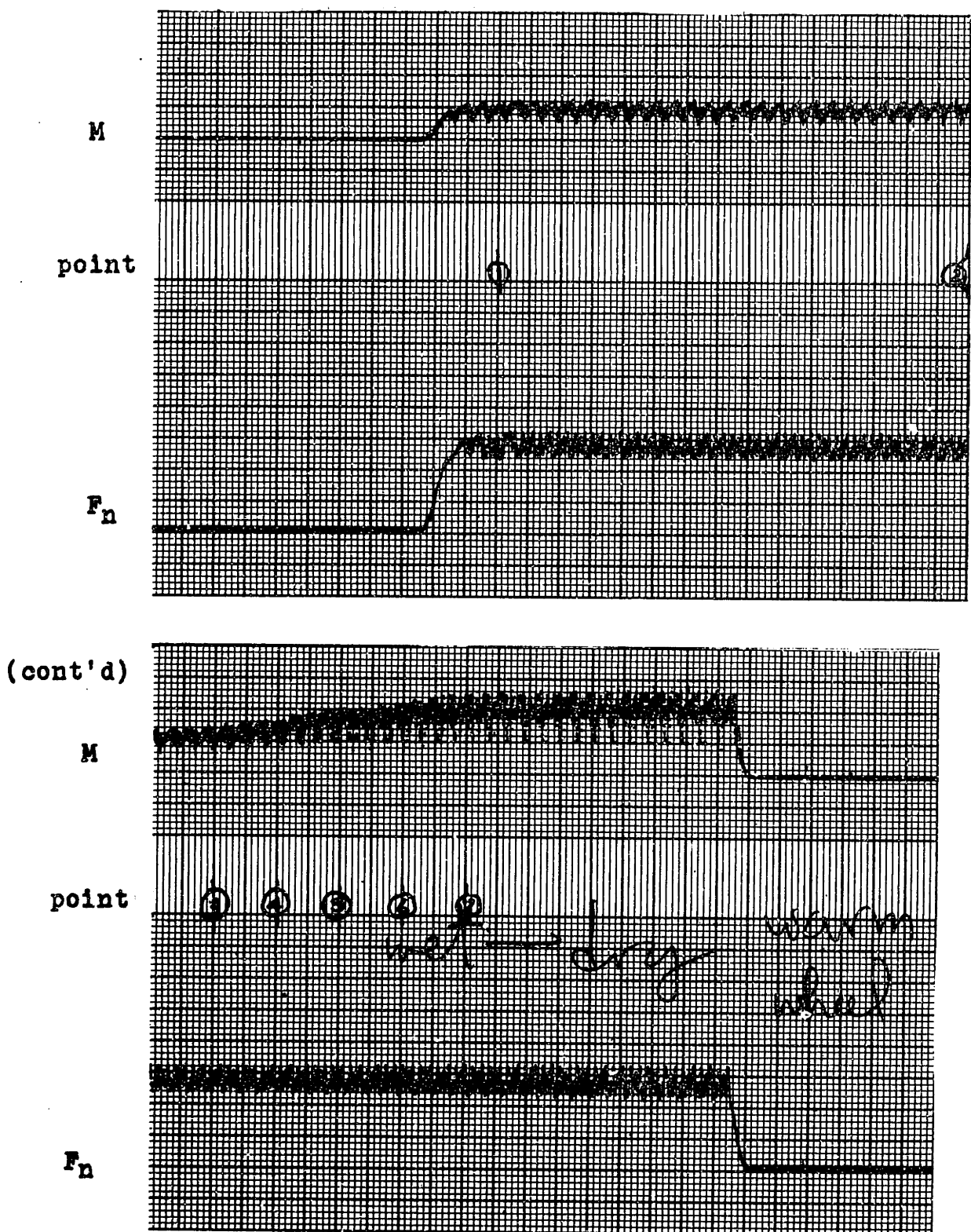


Fig. 10. Graphical output (raw data) for Run C-2.
Friction material: R-451. Wheel speed: 10 mph.
Chart speed: 5 mm/sec.

Appendix C. Table of experimental results

Run	Friction material	Equivalent vehicular speed, mph						
		Nature of run	Average dry coefficient					
			Average wet coefficient					Turns-recovery
			μ_{wet}/μ_{dry}					
			Remarks					
C-1	R-451	10	Dry	.33	--	--	--	$\mu = .39 @ 120^{\circ}F$
C-2	R-451	10	Wet-dry	.34	.17	.50	50	
C-3	B.rubber	10	Wet-dry	.95	.05	.05	55	Erratic recovery
C-4	R-4528-4	10	Wet-dry	.55	.10	.18	54	
C-5	Maple	10	Wet-dry	.44	.09	.20	42	$\mu_{max} = .56$ during rec'y
C-6	Lockheed	10	Wet-dry	.45	.12	.27	25	
C-7	R-451	10	Wet-dry	.34	.17	.50	53	
E-1	Cork A	10	Dry	.63	--			Orientation "A": Layers parallel to friction face
E-2	Cork A	10	Wet	--	.26		.42	
E-3	Cork A	10	Dry	.79	--		.24	
E-4	Cork A	10	Wet	--	.19			
F-1	Cork B	10	Dry	.67	--			Orientation "B": Layers perpendicular to friction face
F-2	Cork B	10	Wet	--	.19		.28	
F-3	Cork A	10	Wet*	--	.16	--	--	
F-4	Cork B	10	Wet*	--	.25	--	--	
F-5	R-451	10	Dry	.43	--	--	--	*48-hr soak
F-6	R-451	10	Wet-dry	.37	.17	.46	70	

Appendix C. Results of friction tests (continued)

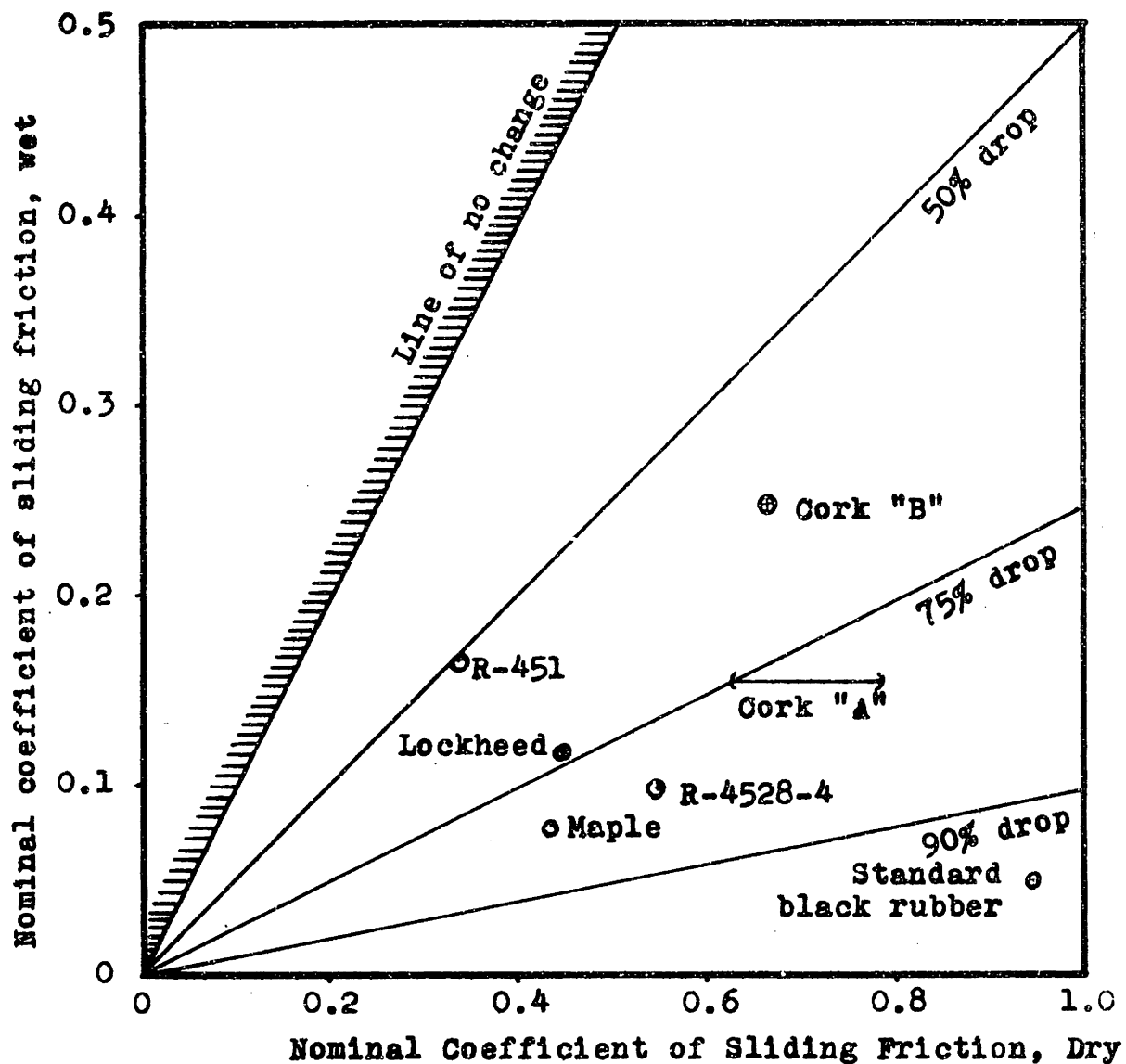


Fig. 11. Wet vs. dry coefficients of sliding friction,
for all friction materials tested,
on nickel-chromium-plated steel wheel rim.

Appendix D. Two representative nonlinear linkages;
Geometric characteristics

1. "Door-closer"

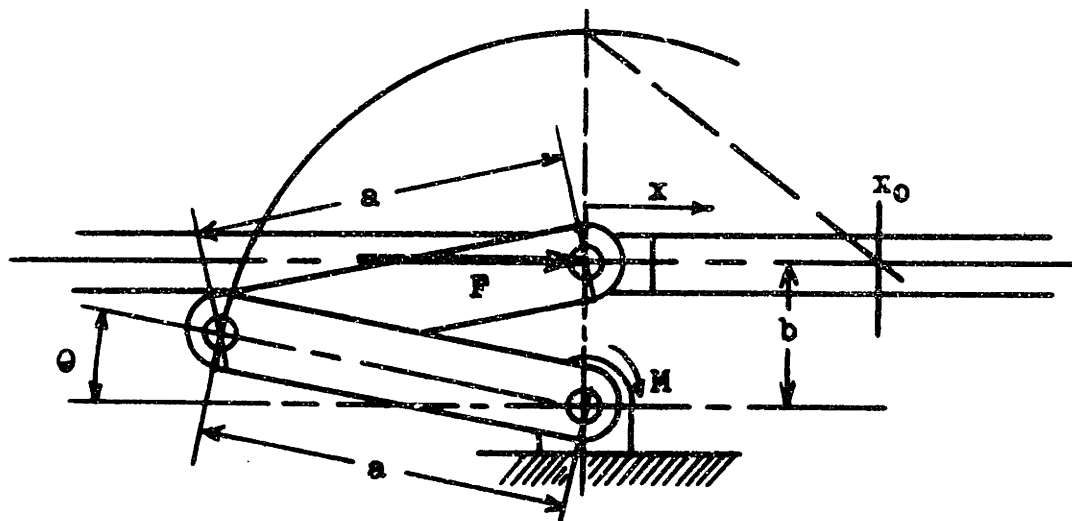


Fig. 12. Geometry of "door-closer" linkage

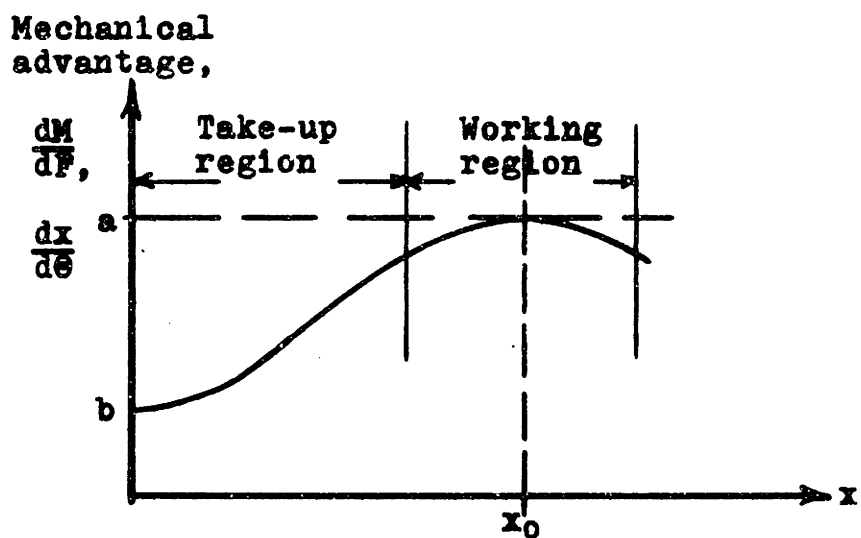


Fig. 13. Approximate characteristics of
 "door-closer" linkage

Appendix D. Representative nonlinear linkages (continued)

2. Stepped-toggle

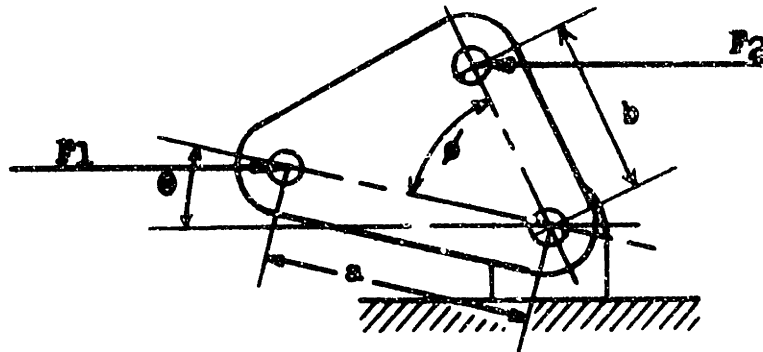


Fig. 14. Geometry of simple toggle

$$\Sigma M_0 = 0,$$

$$F_1 a \sin \theta = F_2 b \sin (\theta + \phi).$$

For F_1 input and F_2 output,

$$\text{mechanical advantage} = \frac{F_2}{F_1} = \left(\frac{a \sin \theta}{b \sin (\theta + \phi)} \right)$$

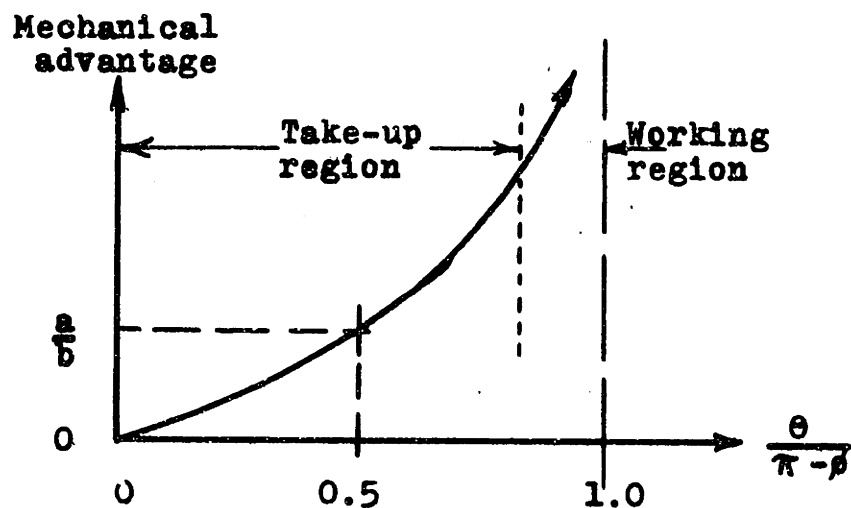


Fig. 15. Mechanical advantage vs. rotation (simple toggle)

Appendix D. Representative nonlinear linkages (continued)

2. Stepped-toggle (continued)

To widen the range of high mechanical advantage, an additional contact point (No. 2) is added to both the toggle and the output link.

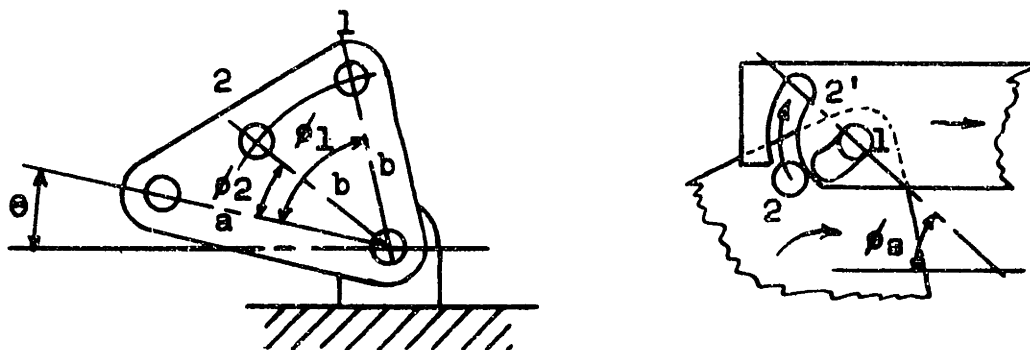


Fig. 16. Geometry of stepped-toggle and output link

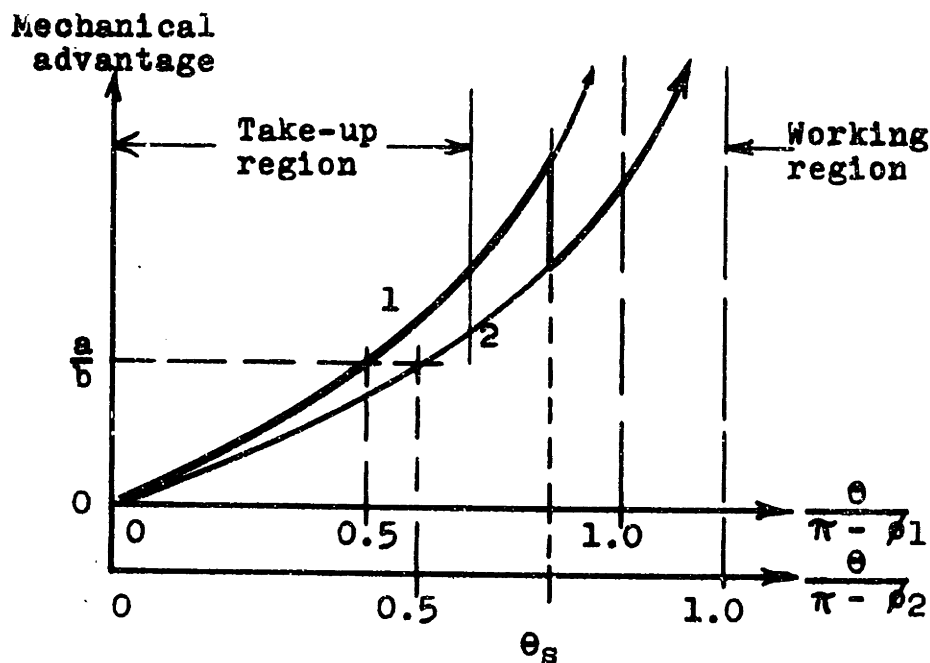


Fig. 17. Mechanical advantage vs. rotation of stepped toggle. Switching occurs at $\theta = \theta_s = \phi_s + \frac{\pi - (\phi_1 + \phi_2)}{2}$.

Appendix E. Servo assist mechanisms

1. Roller-and-screw mechanism with negative force feedback

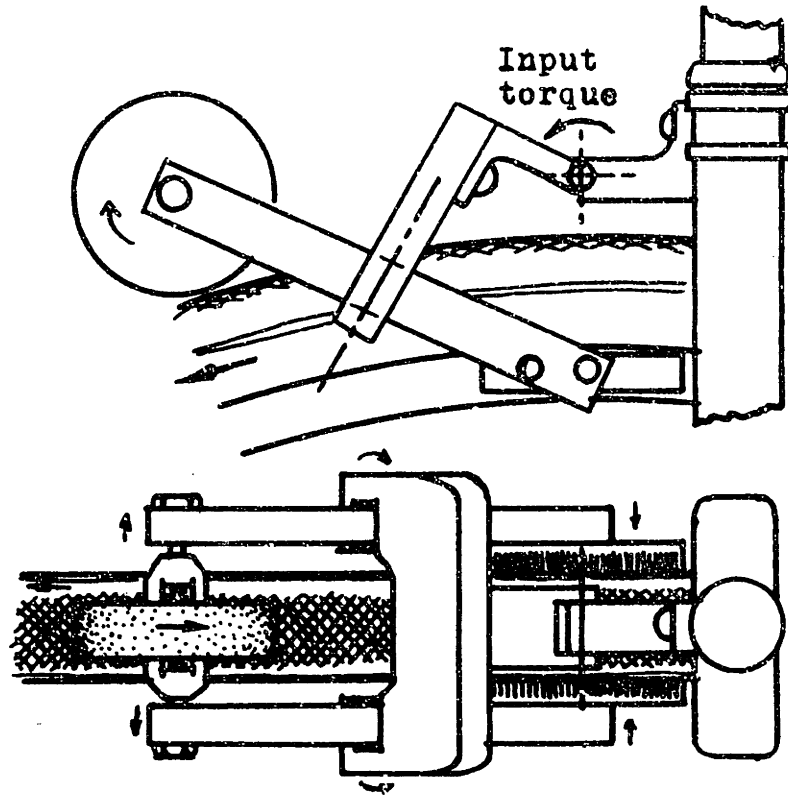


Fig. 18. Roller-and-screw servo. Negative force feedback is accomplished through input torque's being counteracted by moment due to braking force. (See Reference (2), Appendix E, p.31.)

Appendix E. Servo assist mechanisms (continued)

2. Pilot-shoe-and-wedge mechanism, with optional negative force feedback

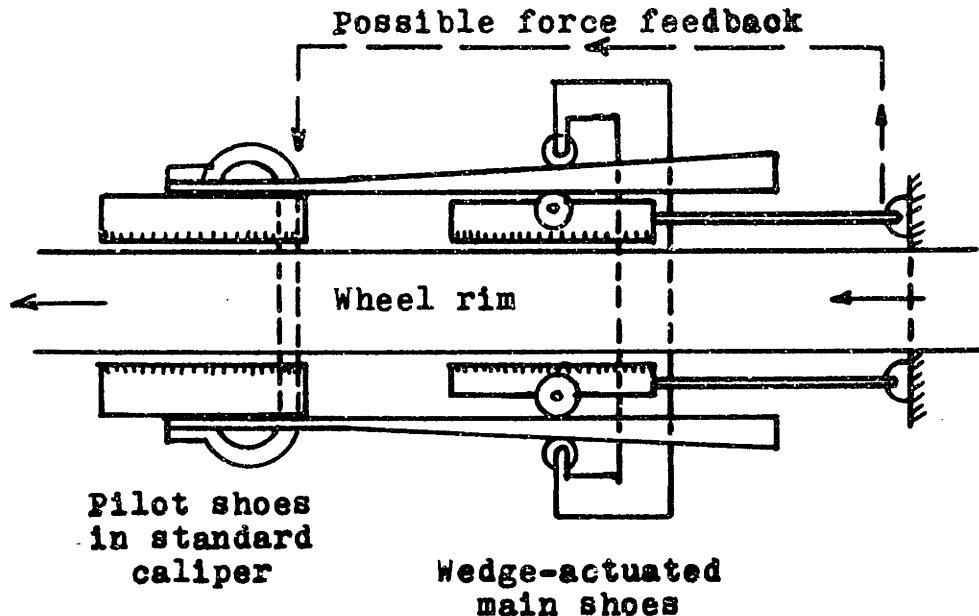
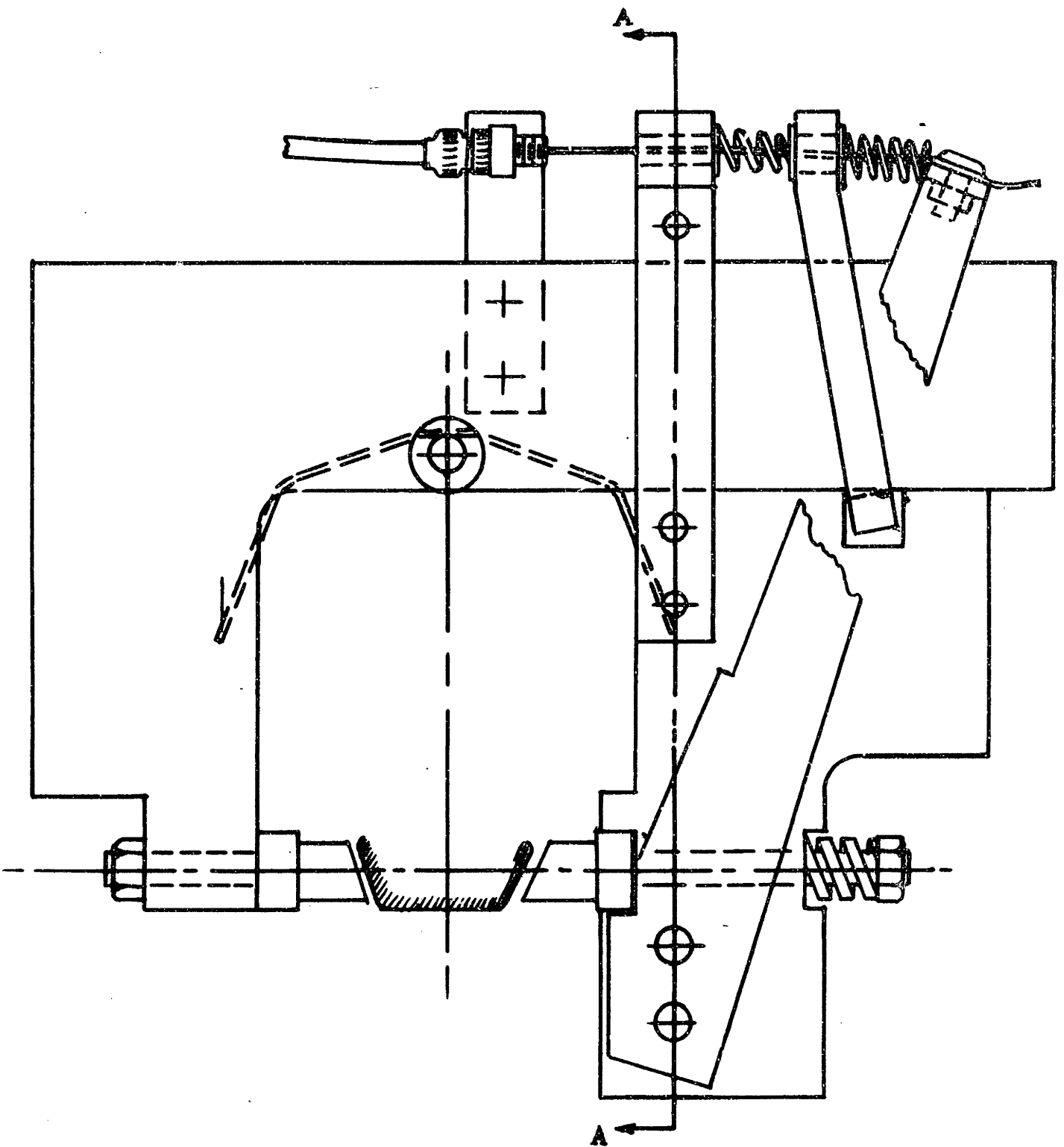


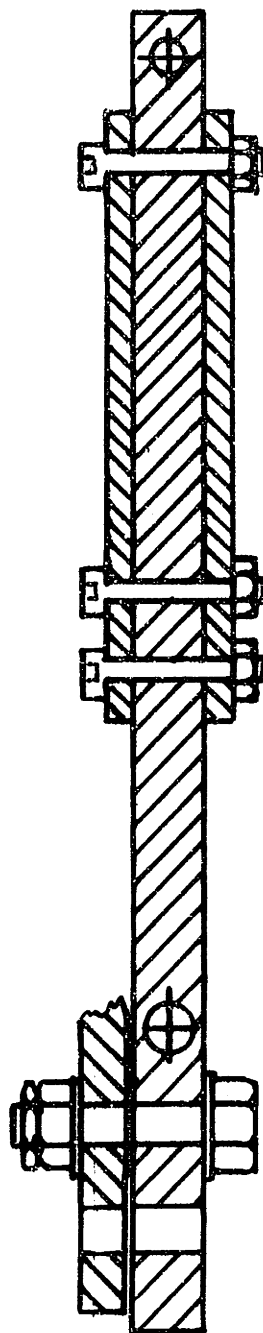
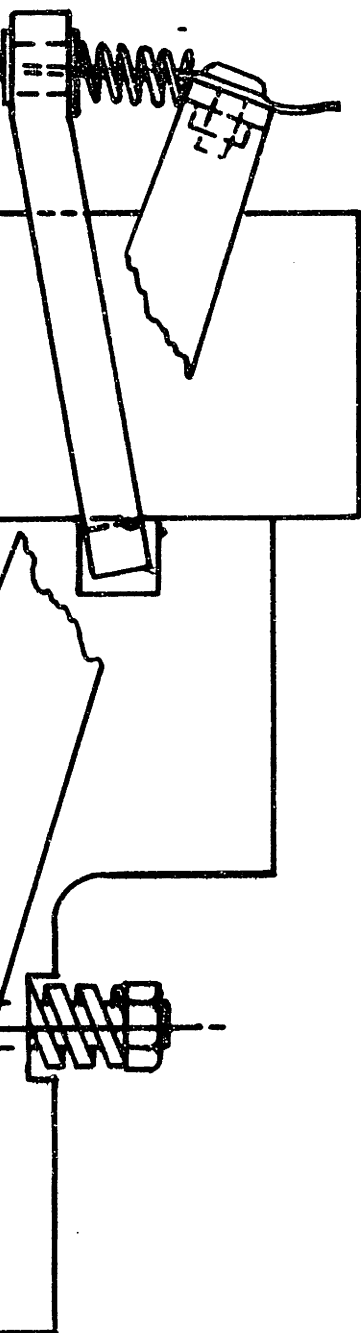
Fig. 19. Schematic diagram of pilot-shoe-and-wedge mechanism. For a total braking force of 100 lbf with an input force of 50 lbf at the pilot caliper and sliding coefficient of 0.15, the required wedge angle ϕ is given by the formula

$$\cot \phi = \left(\frac{F_t}{2\mu^2 F_a} - \frac{1}{\mu} \right) = \left(\frac{1}{.0225} - \frac{1}{.15} \right) = (44\frac{1}{2} - 6\frac{1}{2}) = 38,$$

$$\phi = 1^\circ 30'$$



APPENDIX F: DUAL-MODE MECHANISMS. FIG. 20. FIRST PROTOTYPE.



SEC. A-A

Fig. 20. FIRST PROTOTYPE.

Appendix F. Dual-mode mechanisms (continued)

Geometric requirements for a self-locking, self-releasing link:

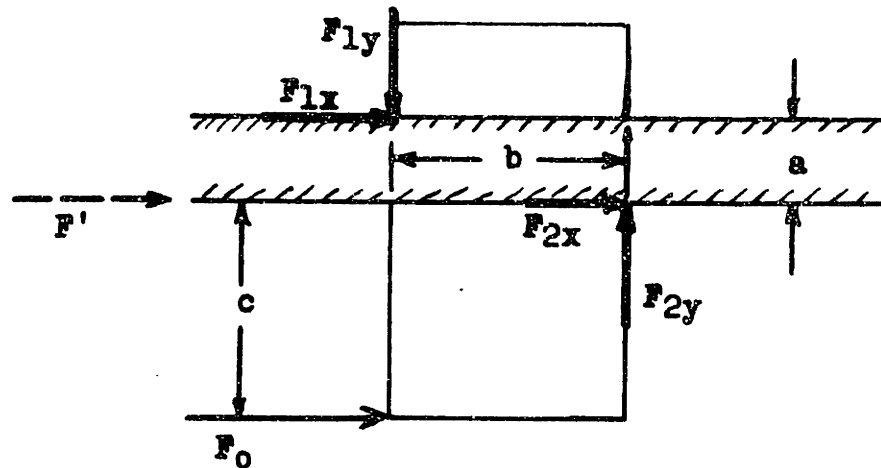


Fig. 21. Forces and geometry of self-locking slider.

The slider is to slide freely when force F' is applied, and lock when force F_0 is applied. This requires that

$$\mu_1 a/2b < 1 \quad (\mu_1 \text{ is static coefficient}),$$

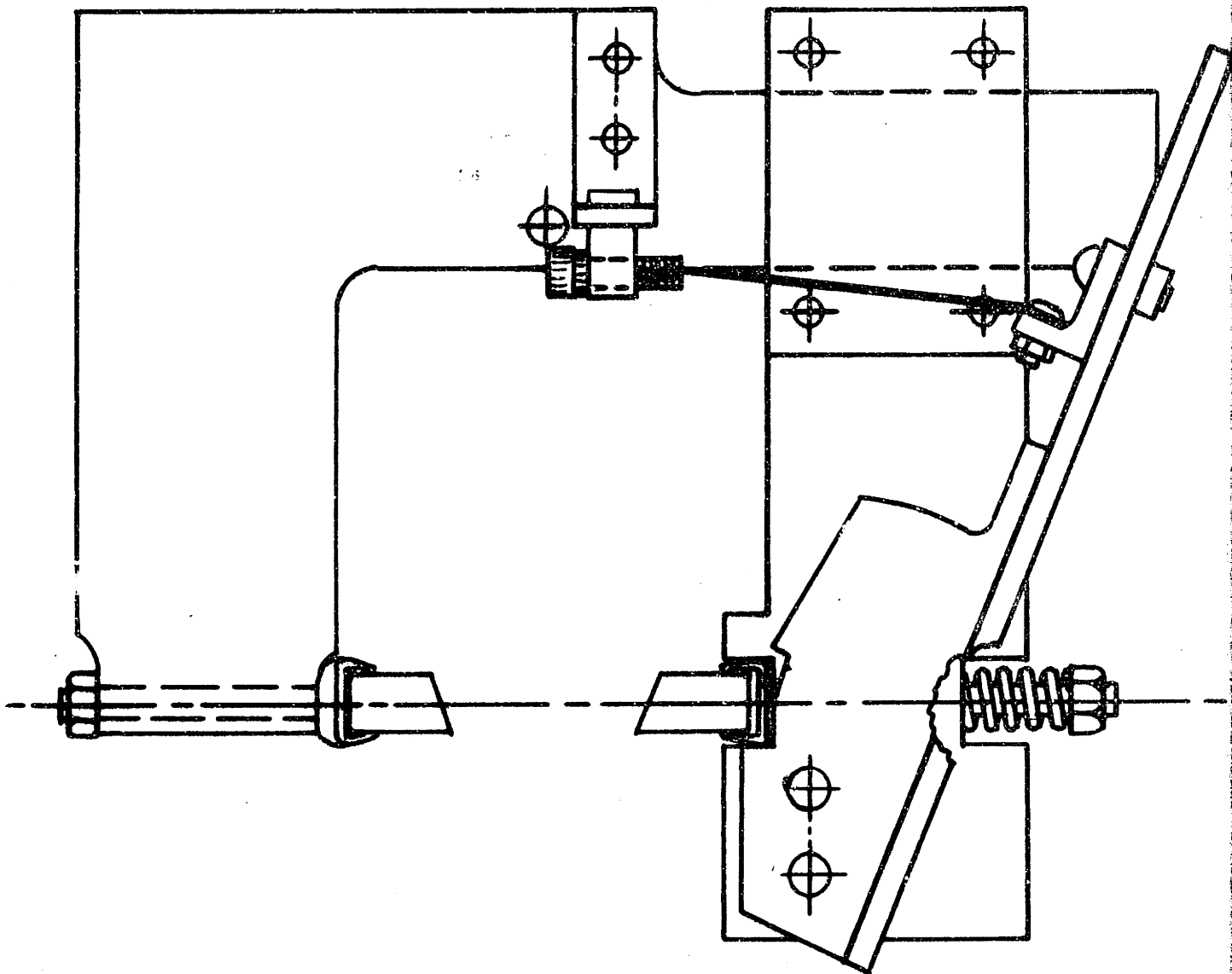
$$\mu_2 \left(\frac{a}{2b} + \frac{c}{b} \right) > 1 \quad (\mu_2 \text{ is sliding coefficient}).$$

For aluminum on aluminum, $\mu_1 = 1.05$ and $\mu_2 = 1.4$ are the published figures.(6) The inequalities become

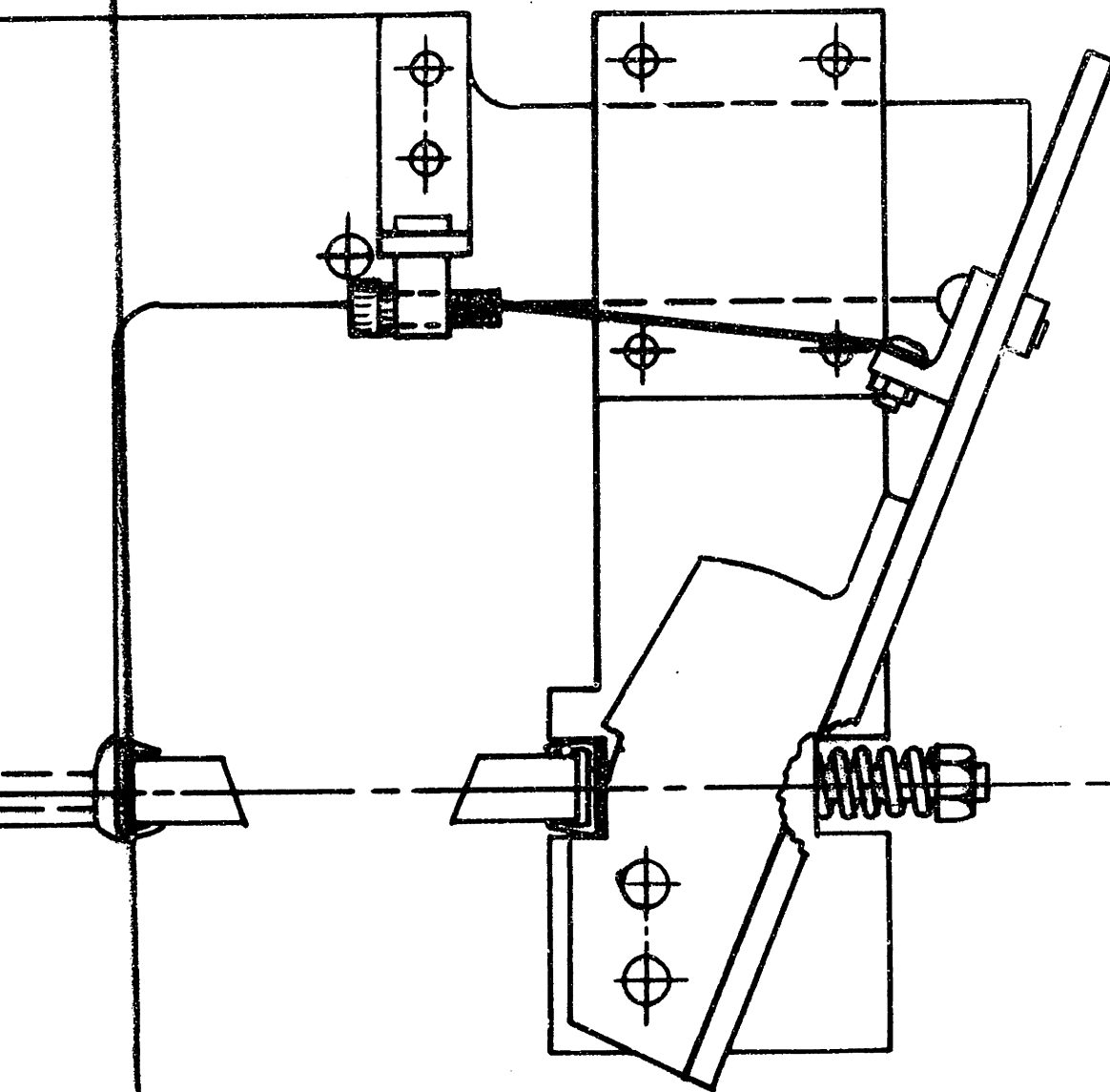
$$\frac{a}{b} < 1.4 ; \quad \frac{a}{2b} + \frac{c}{b} > .95 .$$

which are satisfied by $a/b < 1.4$ and $c/b > 1$.

For the second dual-mode prototype, $a/b = .63$ and $c/b = 1.58$.



APPENDIX F: DUAL-MODE MECHANISMS. FIG. 22. SECOND PROTOTYPE.



MODE MECHANISMS. FIG.22. SECOND PROTOTYPE.